Journal of the European Ceramic Society 20 (2000) 2209–2214

Characterization of a glass-ceramic produced from thermal power plant fly ashes

M. Erol [a], A. Genç [b], M.L. Öveçoğlu [b], E. Yücelen [b], S. Küçükbayrak [a], Y. Taptık [b]

[a] *Department of Chemical Engineering, Chemical and Metallurgical Engineering Faculty, Istanbul Technical University, Maslak 80626, Istanbul, Turkey*

[b] *Department of Metallurgical and Materials Engineering, Chemical and Metallurgical Engineering Faculty, Istanbul Technical University, Maslak 80626, Istanbul, Turkey*

Received 13 December 1999; accepted 19 March 2000

Abstract

Glass-ceramic materials were developed from fly ash samples obtained from Çayırhan Thermal Power Plant in Turkey. On the basis of DTA analyses, nucleation experiments were carried out at 680°C for 5, 10 and 15 h whereas crystallization experiments were performed at 924°C for 20 min. Crystallized samples were cooled in the furnace. X-ray diffraction analyses revealed the presence of only the diopside [$Ca(Mg,Al)(Si,Al)_2O_6$] phase in the produced glass-ceramic samples and scanning electron microscopy (SEM) investigations showed the presence of a homogeneously dispersed phase. The results of the Vickers microhardness tests indicated that the hardness values of the fly ash based glass-ceramic decreased with the increases in holding time at the nucleation temperature. In addition, wear resistance of fly ash-based glass-ceramics decreased with holding time at the nucleation temperature.

Keywords: Fly ash; Glass-ceramics; Mechanical properties; Waste products

1. Introduction

An increasingly urgent problem for the near future is the recycling of industrial by-products and waste materials. Fly ash, a waste product of coal combustion in thermal power plants, is produced in dry form in large quantities (an annual production of 12.5 million tonnes in Turkey[1]) and thus is a major source for environmental pollution. Currently, large quantities of fly ash are used for land-filling which cause negative environmental impacts such as leaching of potentially toxic substances into soils and groundwater, the change in the elemental composition of the vegetation growing in the vicinity of the ash and the accumulation of toxic elements throughout the food chain.[2] For these reasons, the environmental pollution aspect of fly ash should be worked out using both economical and reliable means. Industrial activities pertinent to the utilization of fly ash into useful articles have received worldwide popularity in the last four decades in many areas such as concrete,[1,3–4] brick[5] or cement[6] production. In addition, recent research investigations have reported the use of fly ash to synthesize mullite ceramics,[7] as a raw material for conventional ceramics,[8] for the fabrication of ceramic tableware and artware[9] and for fabricating mineral polymer composites.[10] Although only a small part of the produced fly ash is currently utilized, the largest share of the demand for the fly ash originates from the construction sector.

The physical and chemical properties of fly ash depend on the type of coal used and the combustion conditions. Fly ash exists in different particle sizes (between 1 and 100 μm) and shapes,[2] is made up of tiny glass beads and depending on the chemical composition, its color varies from pale brown to gray. In chemical composition, fly ash consists of oxides such as silica, alumina, calcium oxide, iron oxide and alkali oxides, mostly in glassy states. Due to its complex composition, the melting temperature of fly ash is relatively low.[11] Given these characteristics, fly ash can be vitrified and if it is melted at temperatures above 1300°C, a relatively inert glass is produced.[12] Noting the fact that controlled crystallization can be induced on the vitrified fly ash-based glass, some researchers have recently reported on the utilization of coal fly ashes for the production of

0955-2219/00/$ - see front matter
PII: S0955-2219(00)00099-6

glass-ceramics.[12–15,17] Of all the waste materials, fly ash is probably the most promising material to be utilized for glass-ceramic production considering the overall raw material and production costs.

In this study, the possibility of using waste coal fly ashes in glass-ceramic as a raw material source has been investigated. It is aimed at optimizing the experimental conditions for the development and optimization of glass-ceramic materials from waste coal fly ashes. For this purpose, microstructural characterization and mechanical property investigations were carried out on glass-ceramics devitrified from waste fly ash batches of the Çayırhan thermal power plant.

2. Experimental procedure

2.1. Starting materials

The fly ash batch used in this study was obtained from Çayırhan Thermal Power Plant in Turkey. The chemical analysis showed that the glass forming fly ash consists of the following oxides (in wt.%): 42.82% SiO_2, 16.38% CaO, 5.85% MgO, 7.01% Fe_2O_3, 13.36% Al_2O_3, 5.06% Na_2O, 1.83% K_2O and 6.47 % SO_3. The silica content is within the glass forming region of the SiO_2–CaO–Al_20_3 ternary and falls between the silica content of the fly ash used by Boccaccini et al.[16] and that of the As Pontes fly ash used by Barbieri et al.[17] to form glass-ceramic materials. Fig. 1 is a SEM micrograph of the fly ash sample, showing predominantly spherically shaped powder particles, a typical particle morphology for fly ash powders.[18] Whereas the particle size varies between 1 and 5 μm in size, the average particle size is about 3 μm. Fig. 2 shows the X-ray diffraction pattern of the fly ash sample. As seen in Fig. 2, the as-received fly ash sample comprised the mineral phases: α-quartz (SiO_2), mullite ($Al_6Si_2O_{13}$), enstatite [(Mg,Fe) SiO_3], anorthite ($CaAl_2Si_2O_8$) and hematite (Fe_2O_3). The presence of small amounts of crystalline phases such as quartz and mullite in fly ash batches was also reported by Boccaccini et al.[16]

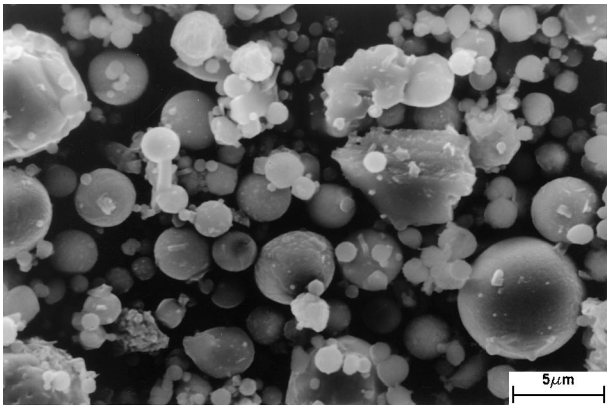

Fig. 1. SEM micrograph of the as-received fly ash.

2.2. Glass-ceramic forming

Fly ash samples were melted in air using Pt-crucibles in an electrically heated furnace at 1400°C for 4 h. No additives or nucleating agents were added to the melting batch. To ensure homogeneity, the melt was poured into water. The cast was crushed, pulverized and remelted at the same temperature for 10 h. Following this, the refined melt was cast in a preheated graphite mould. To remove thermal residual stress, the cast glass was annealed in a furnace at 600°C for 2 h followed by slow cooling to room temperature. The as-cast glass was cylindrical in shape having a diameter of 1 cm and length of 4 cm.

Differential thermal analysis (DTA) scans of as-cast glass specimens were carried out in a Rigaku Thermoflex Thermal Analyzer in order to determine the glass transition temperature (T_g) and the peak crystallization temperature (T_p). After pulverizing and grinding as-cast glass to a powder size of about 30 μm, DTA experiments were performed by heating 100 mg glass powder in a Pt-crucible and using Al_2O_3 as the reference material in the temperature range between 20 and 1100°C at a heating rate of 10°C/min.

Nucleation and crystallization experiments were carried out on the basis of the DTA scan results. For this purpose, small button specimens were sawed from the as-cast fly ash glass sample and these specimens were heated at a rate of 10°C/min to the nucleation temperature of 680°C and held at this temperature for 5, 10 and 15 h. Following nucleation, the temperature was raised to the crystallization temperature of 924°C and held for

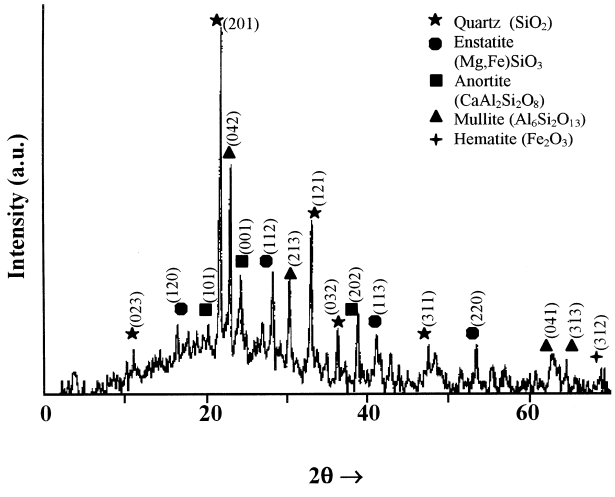

Fig. 2. X-ray diffraction pattern of the as-received fly ash.

20 min. The crystallized samples were cooled in the furnace.

2.3. Microstructural characterization

The microstructural characterization of the as-cast glass and glass-ceramic samples were carried out using both electron microscopy and X-ray diffraction techniques. Scanning electron microscopy (SEM) investigations were conducted in a JEOL™ Model JSM-T330 operated at 25 kV and linked with an energy dispersive (EDS) attachment. For the SEM investigations, optical mount specimens were prepared using standard metallographic techniques followed by chemical etching them in a HF solution (5%) for 1.5 min. The etched optical samples were coated with carbon.

The X-ray diffraction investigations were carried out in a Philips™ Model PW3710 using CuK_α radiation at 40 kV and 40 mV settings in the 2θ range from 0 to 70°. The crystallized phases were identified by comparing the peak positions and intensities with those in the Joint Committee on Powder Diffraction Standards (JCPDS) data files.

2.4. Measurements of mechanical properties

Vickers microhardness measurements of heat treated glass-ceramic samples were made with a LL Model Tukon Tester. Specimens were prepared using conventional metallographic techniques and a load of 500 g were used to indent their surfaces. In order to obtain reliable statistical data, at least 15 indentations were made on each sample. Wear tests were performed in ambient conditions (about 15% humidity) on glass-ceramic specimens machined as cylinders (1×1 cm) using a house-made wear tester. All specimens were wear tested under identical conditions of a rotating 240-grit sandpaper used as the hardfacer. A constant perpendicular load of 20 N and a rotational speed of 0.21 m/s was used throughout the tests. Wear rate values were calculated by measuring the weight loss during the tests.

3. Results and discussion

3.1. Thermal analysis and heat treatment

Differential thermal analysis (DTA) investigations were carried out on as-cast glass samples to determine the nucleation and crystallization temperatures used in producing a glass-ceramic with optimum properties. Fig. 3 shows the DTA thermogram of the as-cast glass sample scanned at the heating rate of 10°C/min. The shallow endothermic peak starting at the onset of 671°C exhibits the glass transition temperature (T_g) and the sharp exothermic peak at 914°C indicates the peak crystallization temperature. These values are very close to those of the low SiO_2 containing 4AP fly ash mixture reported by Barbieri et al.[17] Nucleation and crystallization temperatures were selected 10 °C above the T_g and T_p temperatures as 680 and 924°C, respectively. Preliminary qualitative optical microscopy work was carried out on as-cast glass specimens heated up to 680°C held at different times followed by quenching in air to observe the development of the stable nuclei. Optical samples revealed that stable nuclei formed in the microstructure only after 5 h of holding time at the nucleation temperature. On the basis of this observation, it was decided to carry out the optimization work by changing the holding times at the nucleation temperature but use identical crystallization conditions for all samples. Thus, whereas nucleation times of 5, 10 and 15 h were used, the crystallization conditions were fixed at 924°C/20 min.

3.2. Microstructural characterization

X-ray diffractometry (XRD) scans were carried out on glass-ceramic samples produced by using different heat treatment schemes. In all XRD scans of three devitrified samples produced using different heat treatment, the d-values matched the card values of the diopside-alumina [$Ca(Mg,Al)(Si,Al)_2O_6$] phase. As seen in the representative XRD pattern of the fly ash-based glass-ceramic nucleated at 680°C/10 h (Fig. 4), all the diffraction peaks can be indexed as arising from the reflection planes of the diopside-alumina phase which

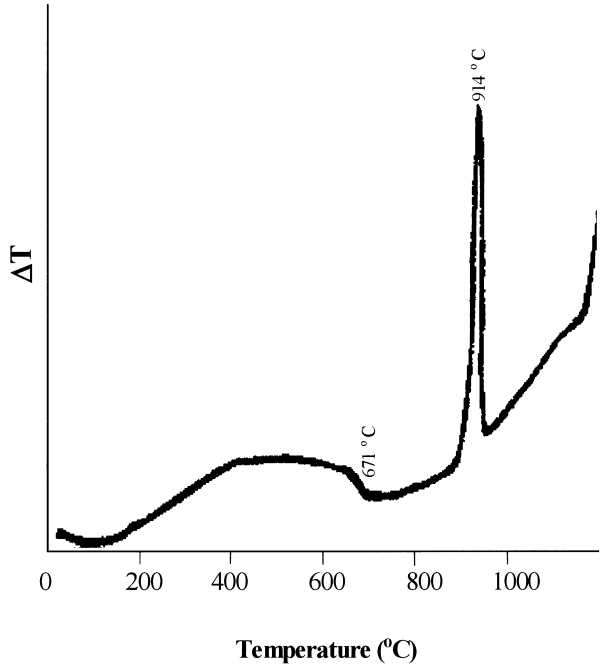

Fig. 3. DTA plot of the as-cast fly ash-based glass.

has a monoclinic structure with lattice parameters $a=0.973$ nm, $b=0.887$ nm, $c=0.528$ nm and $\beta=105.92°$.[19] This is in agreement with the reported literature on glass-ceramics developed from raw materials having similar chemical compositions to the fly ash used in this investigation; either the diopside phase or phases belonging to the diopside group (melilite or akermanite) were reported.[13,20] Baldi et al.[21] and Öveçoğlu et al.[22] also reported the formation of the diopside phase during devitrification in the SiO_2–CaO–MgO ternary at temperatures above 1000 °C.

To investigate the morphology of the resultant microstructure, SEM investigations were conducted on all glass-ceramics. Fig. 5 shows the SEM micrograph of the glass-ceramic sample nucleated at 680°C for 5 h, revealing tiny equiaxed crystallites uniformly dispersed in the microstructure. The average crystalline size is less than 0.25 μm. Fig. 6 is a respective typical SEM micrograph of the fly ash-based glass-ceramic nucleated at 680°C for 10 h. As seen in Fig. 6, the crystallites are uniformly dispersed in the microstructure and the average crystalline grain size is less than 0.5 μm. As a result of increase in the holding time at the nucleation temperature, the average crystalline size for the 10 h sample is larger than that for the 5 h sample. Fig. 7 is a SEM micrograph of the glass-ceramic nucleated at 680°C for 15 h showing the presence of a homogeneous dispersion of equiaxed crystallites about 0.5 μm in size. The crystallites are larger than those of the samples nucleated at 680 °C for 5 and 10 h.

As seen in Figs. 5–7, progressive increases in holding times at the nucleation temperature causes grain growth resulting in larger crystalline sizes in the microstructure. This indicates that the holding times of 10 and 15 h at the nucleation temperature of 680°C are excessively long and that a rather short holding time of 5 h seems to be adequate to form small crystallites in the microstructure. SEM micrographs have also shown that all glass-ceramic samples comprise uniformly dispersed crystallites with grain sizes varying between 0.15 and 0.5 μm with an overall mean grain size of 0.3 μm. This value is better than the mean crystalline size reported by

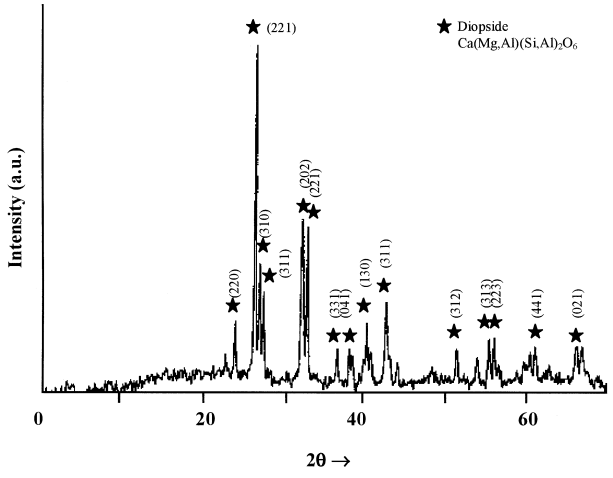

Fig. 4. A representative X-ray diffraction pattern of the fly ash-based glass-ceramic sample.

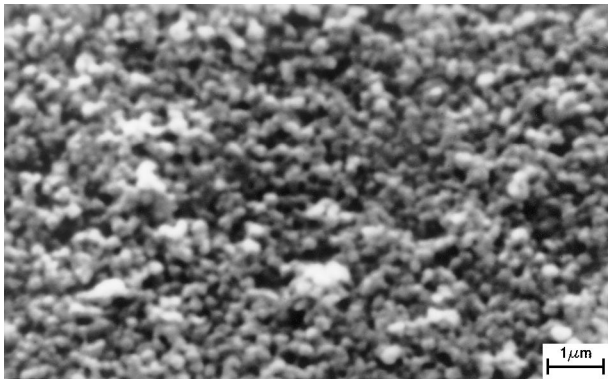

Fig. 6. Representative SEM micrograph of the fly ash-based glass-ceramic nucleated at 680°C for 10 h and crystallized at 924°C for 20 min.

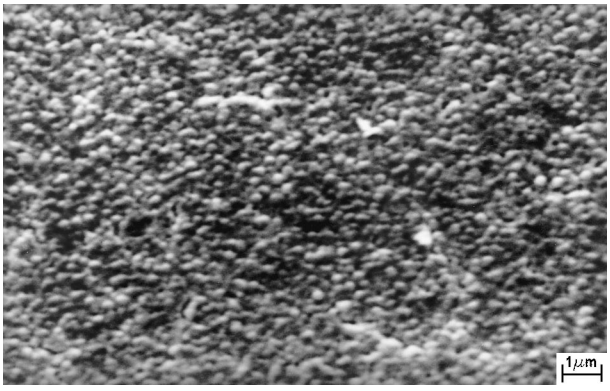

Fig. 5. Representative SEM micrograph of the fly ash-based glass-ceramic nucleated at 680°C for 5 h and crystallized at 924°C for 20 min.

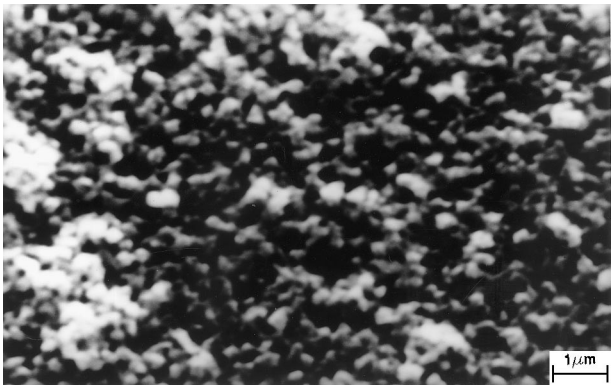

Fig. 7. Representative SEM micrograph of the fly ash-based glass-ceramic nucleated at 680°C for 15 h and crystallized at 924°C for 20 min.

Boccaccini et al.[12] Further, since the controlled heat treatment procedure was applied to all glass-ceramic samples of the present investigation, the crystallites are more uniformly dispersed than those of the glass-ceramic sample (code:4AP) reported by Barbieri et al.[17] In addition, there are no surface cracks observed in the glass-ceramic samples of the present investigation contrary to the glass-ceramic reported by Boccaccini et al.[12]

In order to reveal how the microstructural differences will reflect upon the resultant mechanical properties, mechanical tests such as microhardness and wear were carried out on the fly ash-based glass-ceramics nucleated at different times. In the following section, these properties are presented and evaluated.

3.3. Mechanical properties

Fig. 8 is the error-bar representation of the Vickers microhardness measurements taken from the glass-ceramics nucleated at 680°C for 5, 10 and 15 h. It is quite evident from Fig. 8 that the microhardness values decrease with increase in holding times at the nucleation temperature. In other words, in compliance with the Hall–Petch relation, grain growth at longer holding times account for decreases in microhardness values. Thus, the glass-ceramic sample nucleated at 680°C/5 h has the maximum microhardness value of 907 kg/mm^2 since its grain size is the smallest of all glass-ceramic samples. This hardness value is better than the microhardness values reported by Barbieri et al.[17] and Boccaccini et al.[12] In addition, this value corresponds to about 7.2 in the Mohs' scale and is higher than typical

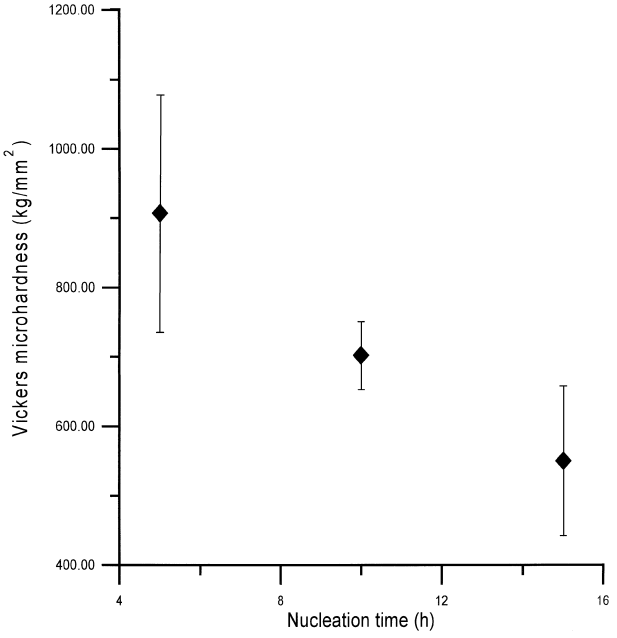

Fig. 8. Vickers microhardness values of the fly ash-based glass-ceramic nucleated at 680°C for 5, 10 and 15 h plotted as a function of the nucleation time.

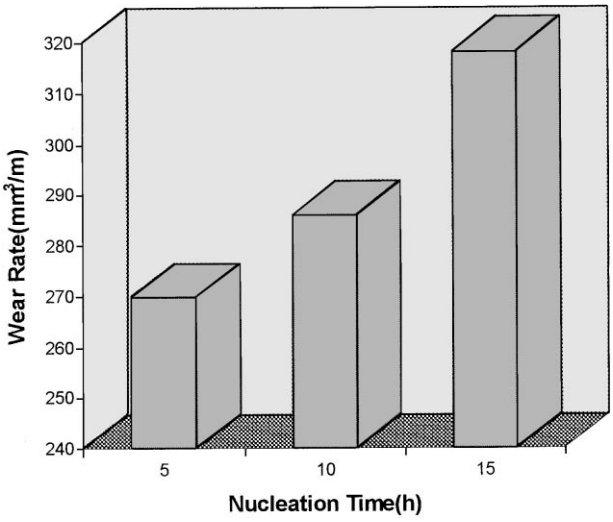

Fig. 9. Wear rate values of the fly ash-based glass-ceramic nucleated at 680°C for 5, 10 and 15 h plotted as a function of the nucleation time.

scratch hardness values for floor tiles which usually range between 5 to 7 Mohs.[23,24] However, it is less than the scratch hardness values reported for slag-based glass-ceramic materials.[25,26]

Fig. 9 is a graphical representation of the wear-rate measurements of fly ash-based glass-ceramics nucleated at 680°C for 5, 10 and 15 h. As seen in Fig. 9, the wear rate increases with the increase in holding time at the nucleation temperature. In other words, the resistance to wear decreases due to grain growth. As the grain boundary area decrease with grain growth, the material becomes more vulnerable to wear. Similar to microhardness results, a maximum resistance to wear is achieved for the fly ash-based glass-ceramic sample nucleated at 680°C/5 h. This is expected since as stated earlier and revealed by the SEM micrograph (Fig. 5), very small ($\leqslant$0.25 μm) grains are present in the sample nucleated at 680°C/5 h.

4. Conclusions

On the basis of the results reported in the present investigation, the following conclusions can be drawn:

1. The crystallization of fly ash-based glasses containing no nucleants takes place at temperatures above 671°C with the formation of only the diopside phase in the parent glass matrix.
2. For all glass-ceramics nucleated at the nucleating temperature of 680°C for different times, the resultant microstructure consists of equiaxed crystallites varying in size between 0.2–0.5 m. The crystalline size increases with the holding time at the nucleation temperature.

3. The progressive increases in the grain size with increases in the holding times at 680°C result in overall decreases in mechanical properties such as microhardness and resistance to wear.
4. The fly ash-based glass-ceramic material with optimum properties for the present investigation is the one nucleated at 680°C for 5 h. This sample has a microhardness value of 907 kg/mm^2 and a wear rate of about 270 mm^3/m.

Overall, results have indicated that fly ash can be used as a raw material to produce glass-ceramic materials and fly ash-based glass-ceramics can be utilized for tiling and cladding applications.

Acknowledgements

The authors would like to acknowledge the help and contribution of Ms. Nurten Dinçer during the SEM investigations of this study.

References

1. Manz, O. E., Worldwide production of coal ash and utilization in concrete and other products. *Fuel*, 1997, **76**(8), 691–696.
2. Carlsson, C. L. and Adriano, D. C., Environmental impacts of coal combustion residues. *Journal of Environmental Quality*, 1993, **22**, 227–247.
3. Anderson, M. and Jackson, G., Beneficiation of power station coal and its use in heavy clay ceramics. *Trans. J. Br. Ceram. Soc.*, 1993, **82**(2), 50–55.
4. Özkan, I., *Effects of Using Fly Ash with Heat Treatments on Concrete Properties*. MS Dissertation Thesis, Istanbul Technical University, Istanbul, Turkey, 1986.
5. Anderson, M., A new low-cost PFA brickmaking process. In *International Conference on Ash Technology*. London, 16–22 September 1984, pp. 569–573
6. Helmuth, R., *Fly Ash in Cement and Concrete*. Portland Cement Association, 1987, p. 203.
7. Hwang, J.-Y., Huang, X. and Hein, A. M., Synthesizing mullite from beneficiated fly ash. *JOM*, 1994, **47**(5), 36–39.
8. Queralt, I., Querol, X., Lopez-Soler, A. and Plana, F., Use of coal fly ash for ceramics : a case study for a large Spanish power station. *Fuel*, 1997, **76**(8), 787–791.
9. Mukherji, S. K. and Machhoya, B. B., The utilization of fly ash in the preparation of ceramic tableware and artware. *British Ceramic Transactions*, 1993, **92**(1), 6–12.
10. Wu, X., Wastiels, J., Faignet, S. and Bauweraerts, P., A composite matrix material based on fly ash. In *Proceedings of International Symposium on Brittle Matrix Composites 4*, ed. A. M. Li, V. C. Li and I. H. Marshall. IKE and Woodhead Publications, Warsaw, 1994, pp. 437–446.
11. Fang, Y., Chen, Y., Silsbee, M. R. and Roy, D. M., Microwave sintering of fly ash. *Materials Letters*, 1996, **27**, 155–159.
12. Boccaccini, A. R., Bücker, M. and Bossrt, J., Glass and glass-ceramic from coal fly-ash and waste glass. *Tile and Brick int.*, 1996, **12**(6), 515–518.
13. Cumston, B., Shadman, F. and Risbud, S., Utilization of coal ash minerals for technological ceramics. *Journal of Materials Science*, 1992, **27**, 1781–1784.
14. Cioffi, R., Pernice, P., Aronne, A., Marotta, A. and Quattroni, G., Nucleation and crystal growth in a fly ash derived glass. *Journal of Materials Science*, 1993, **28**, 6591–6594.
15. Cioffi, R., Pernice, P., Aronne, A., Catauro, M. and Quattroni, G., Glass-ceramics from fly ash with added Li_2O. *Journal of the European Ceramic Society*, 1994, **13**, 143–148.
16. Boccaccini, A. R., Ondracek, G., Janczak, J. and Kern, H., development of composite materials under ecological aspects as recycling concept for coal mining wastes. In *Proceedings of 4th International Symposium on the Reclamation, Treatments and Utilization of Coal Mining Wastes*, Vol. II, ed. K. M. Skarzynska. Krakow, Poland, 1993, pp. 719–726.
17. Barbieri, L., Manfredini, T., Queralt, I., Rincon, J. M. and Romero, M., Vitrification of fly ash from thermal power stations. *Glass Technology*, 1997, **38**(5), 165–170.
18. Boccaccini, A. R., Bücker, M., Bossert, J. and Marszalek, K., Glass matrix composites from coal fly ash and waste glass. *Waste Management*, 1997, **17**(1), 39–45.
19. Powder Diffraction File, Card No. 21-1276, 1992 Database Edition. Joint Committee on Powder Diffraction Standards (JCPDS), Swathmore, PA, USA.
20. Veasey, T. J., Recent developments in the production of glass-ceramics. *Miner. Sci. Eng.*, 1973, **5**(2), 92–107.
21. Baldi, G., Generali, E., Leonelli, C., Manfredi, T., Pellacani, G. C. and Sligardi, C., Effects of nucleating agents on diopside crystallization in new glass-ceramics for tile-glaze application. *J. Mat. Sci.*, 1995, **30**, 3251–3255.
22. Öveçoğlu, M. L., Kuban, B. and Özer, H., Characterization and crystallization kinetics of a diopside-based glass-ceramic developed from glass industry raw materials. *Journal of the European Ceramic Society*, 1997, **17**, 957–962.
23. Tabor, D., The physical meaning of indentation and scratsh hardness. *British J. Appl. Phys.*, 1956, **7**, 159–166.
24. McClintock, F. A. and Argon, A. S., *Mechanical Behavior of Material*. Addison-Wesley, Menlo Park, 1966.
25. Davies, M. W., Kerrison, B., Gross, W. E., Robson, W. J. and Wichell, D. F., Slagceram: a glass-ceramic from blast furnace slag. *Journal of Iron Steel Ins*, 1970, **208**(4), 348–370.
26. Öveçoğlu, M. L., Microstructural characterization and physical properties of a slag-based glass-ceramic crystallized at 950°C and 1100°C. *Journal of the European Ceramic Society*, 1998, **18**, 161–168.